Molecular Cell, Volume *63*

Supplemental Information

Automated Structure- and Sequence-Based Design of Proteins for High Bacterial Expression and Stability

Adi Goldenzweig, Moshe Goldsmith, Shannon E. Hill, Or Gertman, Paola Laurino, Yacov Ashani, Orly Dym, Tamar Unger, Shira Albeck, Jaime Prilusky, Raquel L. Lieberman, Amir Aharoni, Israel Silman, Joel L. Sussman, Dan S. Tawfik, and Sarel J. Fleishman

Supplementary Information

Supplementary figures

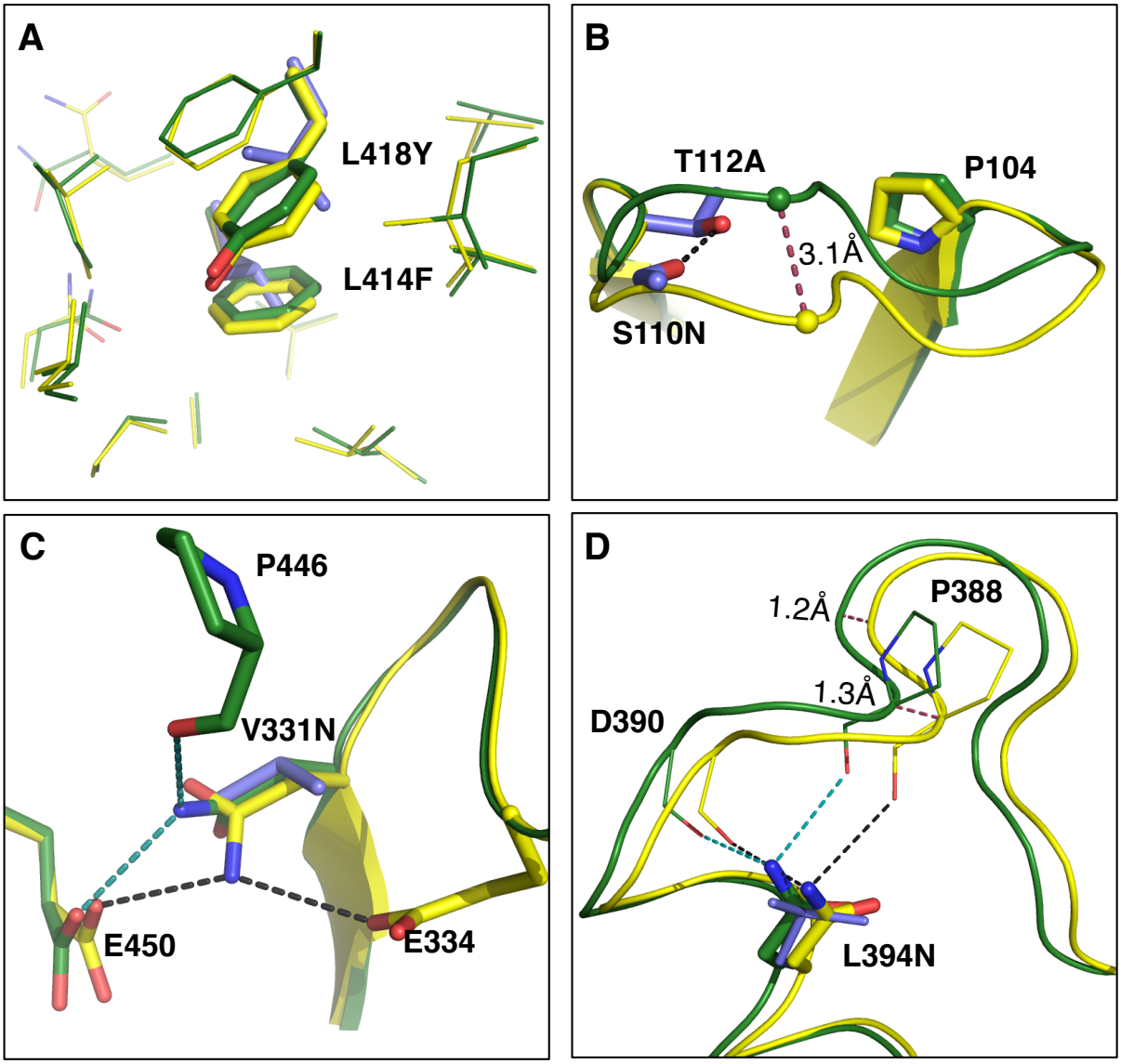

Figure S1. Comparison of the dAChE4 design model (yellow) and the solved crystal structure (PDB entry: 5HQ3, green), Related to Figure 2D. (A) Sub-Ångstrom accuracy in design of two small-to-large core mutations (wild-type leucines are shown in violet). **(B)** The maximal deviation observed between respective Cα atoms in the model and structure is 3.1Å (raspberry dashed line). This conformation change likely results from elimination of a side chain-backbone hydrogen bond between Thr112 and Ser110 due to the designed Thr112Ala mutation. **(C, D)** Comparison of designed buried hydrogen bonds. Val331Asn was predicted to form a hydrogen bond with Glu450 and another with Pro446 in the designed model; in the crystal structure, instead, Asn331 interacts with Glu334 and Glu450 (black and turquoise dashed lines for dAChE4 and the crystal structure hydrogen bonds, respectively; wild-type Val in violet). Leu394Asn forms 2 hydrogen bonds with Pro388 and Asp390, as designed.

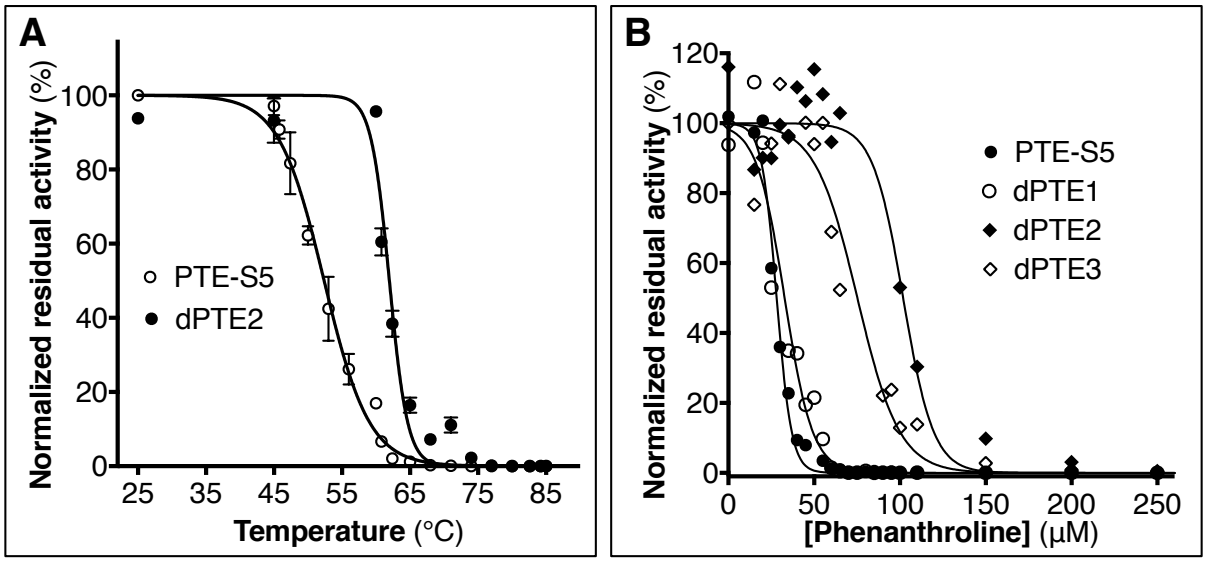

Figure S2. dPTE2 shows higher thermal stability and higher metal cofactor affinity compared to PTE-S5, Related to Figure 3A and Table 3. (A) Residual activities of the purified proteins were measured following incubation at various temperatures on the substrate ethyl-paraoxon. **(B)** Residual activities of the proteins expressed in cell lysates were measured following incubation with various concentrations of a metal chelator, 1,10-phenanthroline.

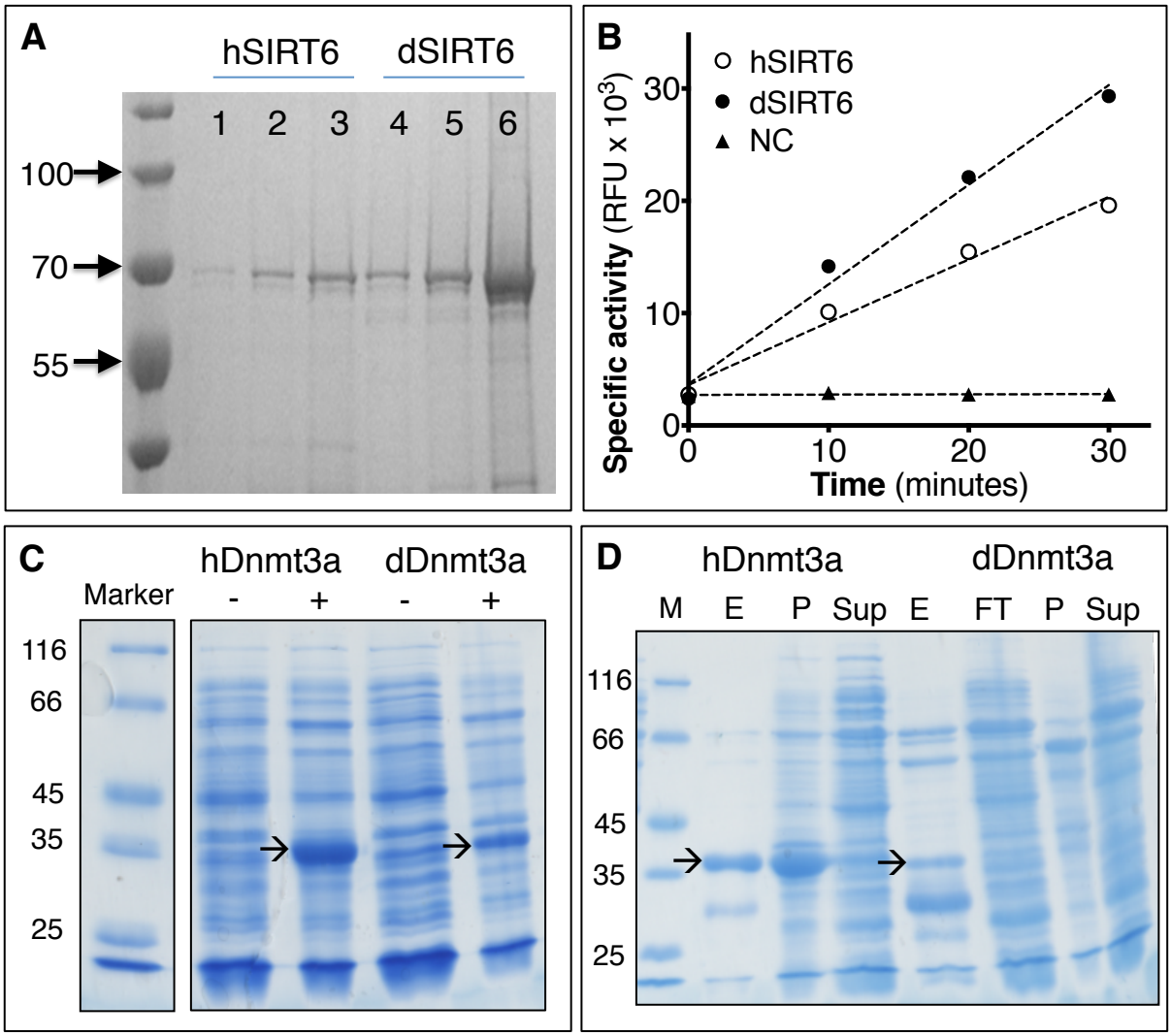

Figure S3. Additional experimental information about SIRT6 and Dnmt3a, Related to Figure 3B & C. (A) dSIRT6 shows fivefold increase in expression relative to hSIRT6. SDS-PAGE shows Ni^{2+}-NTA purified fractions of MBP-fused hSIRT6 and dSIRT6. **(B)** dSIRT6 shows 60% higher activity than hSIRT6. Deacylation activity of purified hSIRT6, dSIRT6 and a negative control (NC) were measured as a function of time. **(C, D)** dDnmt3a shows decreased expression levels compared to hDnmt3a. The left SDS-PAGE shows crude bacterial lysates of hDnmt3a and dDnmt3a before (-) and after induction (+). The right SDS-PAGE shows crude bacterial lysates and purified enzyme samples (E – eluted fraction, P – pellet, Sup – supernatant, FT – flow through). For methylation activity assays, the enzyme concentration was determined by SDS-PAGE comparing various hDnmt3a and dDnmt3a concentrations to a BSA protein standard. The major impurity in the purified dDnmt3a fraction (~30kDa) is an *E. coli* protein, probably prolyl isomerase, that co-elutes with the His-tagged Dnmt3a (Renata Jurkowska, personal communication).

Supplementary Tables

Table S1. False-negative predictions in fungal endoglucanase Cel5A and yeast triosephosphate isomerase (TIM), Related to Figure 1B and Table 1.

Cel5A (PDB entry 3QR3)			
Mutation	**$\Delta\Delta G_{calc}$ (R.e.u.)**	**ΔT_m**	**ΔPSSM[a]**
S133R	-0.14	0.4	-1
K219Q	-0.18	2.8	-4
V101I	-0.28	0.5	1
G239N	-0.33	0.7	-1
S318E	0.14	0.9	-1
S309W	0.29	0.4	5
N155E	0.95	0.5	-2
Y278F	1.05	1.0	-3
T233V	1.27	0.87	2
T80E	1.78	0.5	-4
G293A	1.78	3.7	3
S139P	2.37	2.0	2
I82M	2.71	0.3	0
N76P	3.41	2.0	-1
S318Q	Low PSSM score[b]	0.5	-2
D13E	Low PSSM score[b]	3.0	-4
T18P	Low PSSM score[b]	2.0	-6
F191V	Low PSSM score[b]	0.89	-7
V302A	Low PSSM score[b]	1.0	-4
K219A	Low PSSM score[b]	2.0	-8
S309F	Low PSSM score[b]	2.7	0
S309L	Low PSSM score[b]	1.5	-1
TIM (PDB entry 1YPI)			
I109V	0.70	1.7	1
A66C	1.08	1.9	4
Y49Q	3.42	1.2	-1
I83L	3.59	0.1	1

[a] Difference between the PSSM score of the mutated amino acid and the wild-type amino acid

[b] Mutation showed PSSM score < 0, and was therefore not subjected to Rosetta mutational scanning

Table S2. Modeling constraints, Related to Figures 2 & 3 and Tables 2-4.

Protein (PDB entry)	Unique homologues in MSA	Fixed positions	Reason for fixation/repacking only
hAChE (4EY7)	165	72-79, 82-83, 85-87, 117-122, 124-126, 130, 132-133 202-205, 229, 286-287, 291-297, 334-342, 365, 402, 439, 446-451	8Å from E2020[a]
		373-374, 376-377, 380-381, 383-386, 527, 530, 534, 538-539	5Å from chain B[a]
		256-266, 493-498	Near missing density[b]
		4-7	N terminus[b]
		298	Near catalytic gorge[c,b]
PTE (1HZY)	95	55-60, 100-104, 106, 108, 169-173, 200-202, 230, 233, 253-254, 257, 267, 270-272, 300-303, 305-306, 312-313, 317	8Å from ligand[a,d] (includes also all 5 Å from Zn^{+2} ions)
		61-65, 67-72, 131-141, 145-146, 148-149, 152-153, 159-160, 307-311	5Å from chain B[a]
SIRT6 (3K35)	278	12-13, 15-22, 49-57, 59-65 67-69, 90, 92, 110-113, 130-132, 183-186, 211-218, 220-221, 237-242, 252-259	8Å from APR[a]
		14, 58, 72, 78, 80, 84, 114-115, 134, 139, 141-142, 144, 154, 164, 166, 175, 177, 188-192, 195, 199, 219, 222-223, 225-226, 229, 244, 246-247	5Å from Zn^{+2} ion or peptide[a,e]
		167-174	Near missing density[b]
		291-295	C termini[b]
		66, 155, 210, 243	E1 engineered positions[f]
Dnmt3a (2QRV)	83	635-642, 659-662, 665, 681-684, 702-708, 710-716, 752-756, 777, 783-788, 860, 863-864, 866, 879, 882-890	8Å around SAH or DNA chains[a]
		667, 670-672, 687-689, 719-721, 723, 725-726, 728-729, 731-732, 735-736, 738,740-	5Å from chains B,

		742, 763-764, 767-770, 816-819, 848-849, 851, 853-858, 869, 872-876, 878, 881	D[a]
		823-829	Near missing density[b]
		623-627, 906-908	Termini[b]
		I651F, G669T, H673F, D743P, M775I, M775V, L801Y, P845E, F847T	Post mutation scan exclusion[g]
Myoc-OLF (4WXS/Q/U)	219	None	-

[a] Residues were allowed to minimize but not pack (sample rotamers).

[b] Residues were allowed to pack but not mutate.

[c] Near the catalytic gorge but above the automated fixation cutoffs.

[d] Ligand is DPJ from PDB entry 4NP7.

[e] Peptide is chain F from PDB entry 3ZG6.

[f] Positions engineered by authors O.G. and A.A. to generate the variant E1 (data not published)

[g] Mutations with exceptionally large difference in Rosetta omega dihedral energy were excluded.

Table S3. Computational parameters used to generate design variants, Related to Figures 2 & 3 and Tables 2-4.

Stabilization target	# designs	$\Delta\Delta G_{calc}$ cutoffs[a] (R.e.u.)
AChE	5	-2.0 (17), -1. 5 (30), -1.0 (42), -0.75 (51), -0.45 (67)
PTE	3	-2.0 (9), -1.0 (19), -0.45 (28)
Dnmt3a	1	-0.45 (14)
SIRT6	1	-0.45 (11)
Myoc-OLF	1	Combined mutations from analysis of design output using 3 PDB entries: 4WXS, 4WXQ, 4WXU (21)

[a] Cutoffs used to define the spaces of potentially stabilizing mutations in computational mutation scanning. Each defined space resulted in a single final variant that was experimentally tested. In Figures in parentheses show the number of mutations relative to starting sequence obtained by each cutoff in the final variant.

Table S4. Production and purification of AChE variants from 250 ml cultures, Related to Figure 2 and Table 2.

Protein	**Mutations relative to hAChE**	**Final Volume (µl)[a]**	**Concentration from activity (µM)[b]**	**% Purity by PAGE gel[c]**	**Yield (µg/ liter culture)**
hAChE[d]	-	850	0.000312	ND[f]	0.064
dAChE1	17	750	1.0102	34	219.2
dAChE2	30	200	0.56	31	121.2
dAChE3	42	350	1.02	72	395.2
dAChE4[e]	51	23000	0.0345	53	1974.8
dAChE5	67	200	0.92	75	118.4

a. Final volume of a pure protein solution obtained from a 250ml *E. coli* culture expressing the protein, after concentration

b. Active AChE protein concentrations obtained from activity measurements on ACh

c. AChE protein purity estimated by quantification of the 60kDa bands in SDS-PAGE gels

d. The purity and yield of hAChE expressed in *E. coli* cells (see extended experimental procedures) were very low relative to other variants

e. This variant was not concentrated following purification

f. Not determined

Table S5. Data collection and refinement statistics for dAChE4 crystallographic analysis, Related to Figure 2D.

Data collection	**dAChE4**
PDB code	5HQ3
Space group	$P4_32_12$
Cell dimensions:	
a,b,c (Å)	89.53, 89.53, 395.30
a,b,g (º)	90, 90, 90
No. of copies in a.u.	2
Resolution (Å)	49.42-.2.60
Upper resolution shell (Å)	2.74-2.60
Unique reflections	50786(7238)*
Completeness (%)	99.9 (99.8)
Multiplicity	9.7(9.9)
Average I / s(I)	6.1 (1.3)
R_{sym} (I) (%)	10.7 (57.6)
Refinement	
Resolution range (Å)	49.42-2.60
No. of reflections (I/s(I) > 0)	48279
No. of reflections in test set	2498
R-working (%) / R-free (%)	20.5 / 25.4
No. of protein atoms	8316
No. of ions/ligands atoms	36
No. of water molecules	1
Overall average B factor ($Å^2$)	41.0
Root mean square deviations:	
- bond length (Å)	0.019
- bond angle (°)	1.956
Ramachandran Plot	
Most favored (%)	88.9
Additionally allowed (%)	10.3
Disallowed (%)	0.2

* Values in parentheses refer to the data of the corresponding upper resolution shell

Table S6. Expression levels and thermal stabilities of Myoc-OLF variants, Related to Figure 3D & E.

Protein Variant	Mutations	Expression[a]	T_m (°C)
hMyoc-OLF	--	2 mg / L	53.0 ± 0.5[b]
hMyoc-OLF + 10mM $CaCl_2$	--	--	59.6 ± 0.2[b]
dMyoc-OLF	21	19 mg / L	69.8 ± 0.8
dMyoc-OLF + 10mM $CaCl_2$	21	--	73.4 ± 0.5

[a] Expression levels quantified by yield of cleaved purified myoc-OLF per liter of cell culture.

[b] Values taken from Donegan *et al*.(Donegan et al., 2012)

Data S1. RosettaScripts, flags and command lines, Related to Experimental procedures.

Data S2. Protein and DNA sequences of experimentally tested constructs, Related to Experimental procedures.

Extended experimental procedures

Experimental procedures

For RosettaScripts, flags, and command lines see **Data S1.**

DNA and protein sequences of all tested designs and their wild-type counterparts are provided in a supplemental file **Data S2**.

Cloning, expression, and purification of AChE variants

The hAChE gene (Uniprot P22303), without its 31aa N-terminal signal-peptide and its 34aa C-terminal tetramerization domain (ORF length 1,647bp), was codon-optimized for expression in *E. coli* and synthesized (Gen9, Boston). The designed hAChE variants were similarly constructed, codon-optimized and synthesized **(Data S2)**. The synthetic genes were cloned into a pET32b+ vector (Novagen, Darmstadt, Germany) in fusion with an N-terminal TRX tag, using *NcoI* and *XhoI* restriction sites. The ligated plasmids were transformed into *E. coli.* SHuffleT7Express cells (NEB, Ipswich, Massachusetts) for expression.

Single colonies expressing hAChE or its designed variants were used to inoculate starter liquid cultures (2YT plus ampicillin (100mg/l) and spectinomycin (100mg/l)) that were grown O/N at 37°C. These were used to inoculate similar cultures of 250ml, grown to OD_{600nm}= 0.5, induced with IPTG (0.45mM) and grown at 20°C for 24 h. Cells were pelleted, dried, frozen at -80°C and lysed by addition of 40ml lysis buffer (20mM Tris-HCl pH 8.0; 100mM NaCl; 10% glycerol; 0.4mg/ml lysozyme; 50U benzonase (Sigma, St. Louis); 10mM EDTA). Lysates were incubated for 15min at 37°C, sonicated (5x 30", 35% amplitude, Sonics-Vibracell VCX750), and then N-octylglucoside (0.1% W/V) and 100 ml of buffer B (10 mM Tris-HCl pH 8.0; 10% glycerol; 10 mM EDTA) were added, and the debris was pelleted. The clarified lysates were loaded onto an affinity column consisting of the affinity ligand *m*-aminophenyltrimethylammonium coupled to Sepharose 4B via a dicaproyl spacer(Sussman et al., 1988); 1ml resin/50ml culture, washed with buffer A (20mM Tris-HCl, pH 8; 30mM NaCl; 10% glycerol; 0.1% N-octylglucoside; 10mM EDTA), and eluted with buffer A supplemented with 50mM tetramethylammonium bromide plus 40mM NaCl. Fractions containing AChE were pooled, concentrated and dialyzed against dialysis buffer (20mM phosphate buffered saline, 10% glycerol, 0.1% N-octylglucoside). Protein

concentration was determined using the BCA assay (Pierce, Waltham, Massachusetts) and purity was assessed by SDS-PAGE.

AChE activity assays in bacterial cell lysates

Transformed *E. coli* colonies (as above) were picked into 96 deep-well plates containing 0.5ml 2YT plus ampicillin and spectinomycin (100 mg/l each), grown to OD_{600nm}=0.5, induced with IPTG (0.45mM), and grown at 20°C for 24 h, followed by 14 h at 16°C. Cells were pelleted, dried and frozen at -80°C. Lysis buffer containing 0.1% v/v Triton X-100 was added (300µl/well), plates were placed in a shaker-incubator (37°C, 1.5 h, 1200 RPM) and the resulting lysates were clarified by centrifugation. Samples of 10µl clear lysates were transferred to Greiner 96-well ELISA plates (Sigma, St. Louis) for activity assays. AChE activity was measured by the addition of 190µl of Ellman's reagent (0.85mM DTNB; Sigma, St. Louis), 0.55mM acetylthiocholine (Sigma, St. Louis), in PBS). Initial velocities were recorded at 412nm using a plate-reading spectrophotometer (PowerWave HT, BioTek, Winooski, Vermont).

Heat inactivation of hAChE designs

E. coli cells, expressing hAChE or its designs, were grown and lysed as described above. Samples of 20µl of clear cell lysates were transferred to a 96-well PCR plate (Axygen, Corning) using a Precision-2000 liquid handler (BioTek, Winooski), incubated in a gradient PCR (Biometra, Göttingen, Germany) for 30min at various temperatures and cooled to 4°C (10min). Samples of 10µl were transferred to 96-well ELISA plates and their AChE activity was measured as described above. The inactivation temperature (denoted as T_m) of the expressed enzymes was calculated by fitting its residual room-temp AChE activity at different temperatures to a 4-parameter Boltzmann sigmoidal curve: $A_t = A_0 + \frac{A_f - A_0}{1+e^{(Tm-T)/m}}$ where A_t corresponds to the residual activity following incubation at a given temperature T, A_0 is the activity of the unheated sample at room temperature, A_f is the activity at maximal inactivating temperature, and m is the sigmoidal slope coefficient. The heat inactivation of purified proteins was similarly measured. For heat-inactivation assays of purified proteins, hAChE (positions 32-574) was cloned in the pHLsec expression vector(Aricescu et al., 2006) and produced in large scale in HEK293T cells. The secreted protein was purified from the medium by affinity chromatography(Sussman et al., 1988) and deglycoasylated with PNGase F.

Determination of AChE kinetic parameters

Purified hAChE or designed variants were diluted in activity buffer (20mM PBS, pH 7.4, 0.1% BSA) (Sigma, St. Louis) to 0.5-3nM. Increasing amounts of the toxic isomer of the organophosphate nerve agent VX (*i.e.* S_P-VX; details of synthesis may be provided upon request) were added up to inhibition of 90% of the initial AChE activity. Residual AChE activity of aliquots was monitored using the Ellman protocol(Ellman et al., 1961). The concentration of AChE active sites was determined by plotting residual AChE activity *versus* S_P-VX concentration and extrapolating to zero AChE activity. V_{max} and K_M were determined in 50mM PBS pH 8.0 at 25^{o}C, by measuring initial velocities of acetylthiocholine hydrolysis (at 0.02 to 0.4mM acetylthiocholine (Sigma, St. Louis)) during the first 1.5min and fitting the data to the Henri-Michaelis-Menten equation(Segel, 1976). k_{cat} was calculated by dividing V_{max} by AChE active-site concentration.

dAChE4 production and purification for X-ray crystallography

Trx-dAChE4 (in *E. coli* SHuffleT7Express cells) was produced in 7.5L LB medium. Cells were grown at 30^{o}C until they reached A_{600}=0.5, and induced with 0.5 mM IPTG for 24 h at 20^{o}C. The published purification protocol for hAChE(Sussman et al., 1988) was modified as follows: The cell pellet was resuspended in lysis buffer (20mM Tris pH 8.0, 100mM NaCl, 10% glycerol, 0.2mg/ml lysozyme, 10mM EDTA, 1μg /ml DNAse) and disrupted by a cell disrupter at 4^{o}C. 0.1% (w/v) *N*-octyl glucoside was added to the cleared lysate and left to rotate for 1 h at 4^{o}C. The solution was diluted by adding 2.5x volumes of buffer (20mM Tris pH 8.0, 10% glycerol, 10mM EDTA and 0.1% (w/v) *N*-octyl glucoside) and clarified by centrifugation at 15,000 g for 30min. Trx-dAChE4 was purified on an affinity column consisting of the ligand (*m*-aminophenyl)trimethylammonium coupled to Sepharose 2B (Pharmacia) (prepared by Lilly Toker according to the manufacturer's instructions). After loading the clarified lysate, the column was washed with buffer containing 20mM Tris pH 8.0, 30mM NaCl, 10% glycerol, 10mM EDTA and 0.1% (w/v) *N*-octyl glucoside, and the enzyme was eluted with the same buffer containing 50mM tetramethylammonium bromide. Fractions containing Trx-dAChE4 were pooled and concentrated before injecting onto a Superdex 200 HR 10/30 column (GE Healthcare) equilibrated with 50mM Tris pH 8.0, 100mM NaCl. Trx-dAChE4 was concentrated to 10 mg/ml for crystallization. Spontaneous cleavage of the Trx occurred during the process.

Structure determination and refinement of dAChE4

Crystals of dAChE4 were obtained using the sitting-drop vapor-diffusion method with a Mosquito robot (TTP LabTech). The crystals were grown from 8% PEG 6000, 0.1M $MgCl_2$ and 0.1M MES pH 6.0. The crystals formed in the tetragonal space group $P4_32_12$, with 2 monomers per asymmetric unit. A complete dataset to 2.6 Å resolution was collected at 100 K using a single crystal on beamline BM14 of the European Synchrotron Radiation Facility (ESRF, Grenoble). Diffraction images were indexed and integrated using Mosflm(Leslie and Powell, 2007), and the integrated reflections were scaled using SCALA(Evans, 2006). Structure-factor amplitudes were calculated using TRUNCATE (CCP4 program suite)(French and Wilson, 1978). The structure was solved with PHASER(McCoy, 2006) using the refined structure of hAChE (PDB entry: 4EY4(Cheung et al., 2012)) as a molecular-replacement model. All atomic-refinement steps were carried out with CCP4/REFMAC5(Murshudov et al., 1997). The model was built into $2mF_{obs}$ - DF_{calc}, and mF_{obs} - DF_{calc} maps using COOT(Emsley and Cowtan, 2004). The R_{free} value is 25.4% (for the 5% of reflections not used in the refinement), and the R_{work} value is 20.5 % for all data to 2.6 Å. The dAChE4 model was evaluated with MOLPROBITY(Chen et al., 2010). Details of the refinement statistics are described in **Table S5**. The coordinates of dAChE4 were deposited in the RCSB Protein Data Bank as entry 5HQ3.

AChE inhibition by S_P-VX

The concentration of the toxic enantiomer (S_P) of VX [*O*-ethyl *S*-(2-(diisopropylaminoethyl) methylphosphonothioate] was determined by monitoring thiol released in the presence of NaF, and verified by use of the PTE variant C23(Cherny et al., 2013). The pseudo first-order rate constant (k_{obs}) for hAChE inhibition (0.2-1nM in activity buffer) by ≥10-fold stoichiometric excess of S_P-VX increased linearly with increasing S_P-VX. Since the inhibitor concentration was well below what would be expected from the dissociation constant of its reversible complex with hAChE(Berman and Leonard, 1989), the second-order rate constant for inhibition was obtained by dividing k_{obs} by S_P-VX concentration.

PTE activity assays in bacterial cell lysates

E.coli GG48 cells(Grass et al., 2001) expressing PTE-S5 or its designed variants were plated on LB plus ampicillin(100mg/l) plus kanamycin(50mg/l) agar, and grown overnight at 37°C. Colonies were randomly picked into 96 deep-well plates (Axygen, Union City, California)

containing 0.5ml 2YT plus ampicillin (100mg/l) and kanamycin (50mg/l), grown to OD_{600nm}=0.5, induced by adding IPTG (0.5mM, final concentration), and further grown at 20°C for 24 h. The cells were then pelleted, dried, and frozen at -80°C. Plates were defrosted at room temperature, and cells were lysed by addition of lysis buffer (0.1M Tris-HCl pH 8.0, 0.1M NaCl 1, 0.1% Triton X-100; 10mM Na_2CO_3, 0.2mg/ml lysozyme and 50U benzonase nuclease) followed by incubation in a shaker-incubator at 37°C, for 1.5 h at 1200 RPM. Lysates were clarified by centrifugation. Samples of clear lysates were diluted 1:200 in PTE activity buffer, and 5µl dilute samples were transferred to Greiner 96-well plates (Sigma, St. Louis) for activity assays. PTE activity on paraoxonase was measured by addition of 195µl, 0.2mM paraoxon in 0.1M Tris pH 8.0, plus 0.1M NaCl. Initial velocities were recorded at 405nm using a plate-reading spectrophotometer (PowerWave HT, BioTek, Winooski, Vermont).

PTE heat-inactivation temperature and metal-binding affinity

Heat-inactivation temperature was assayed as described above for AChE, except that residual activity was measured using paraoxon as substrate (described above). Residual activity at increasing concentrations of the metal-binding chelator 1,10-phenanthroline was assayed as described(Roodveldt and Tawfik, 2005). Briefly, clarified cell lysates were incubated for 90 min at room temperature with 10-500µM of 1,10-phenanthroline. All samples, including the untreated sample, contained up to 0.5% methanol. The samples were subsequently diluted 1:200 in activity buffer, incubated for 30 min at room temperature, and assayed with 0.25mM paraoxon. Data were fit to a 4-parameter Boltzmann sigmoid: $A_c = A_0 + \frac{A_f - A_0}{1+e^{(C_m - C)/m}}$ where A_c corresponds to the residual activity following incubation at a given 1,10-phenanthroline concentration, C, A_0 is the activity of the sample without 1,10-phenanthroline, A_f is the activity at maximal 1,10-phenanthroline concentration, C_m , is the mid-inactivation concentration, and *m* is the sigmoidal slope coefficient. Residual activity as a function of the time of incubation with 1,10-phenanthroline was assayed at 0.25µM PTE (wild-type-like PTE-S5, or the designed variant, PTE-dPTE2) and 50µM 1,10-phenantroline at room temperature. Aliquots were removed at various time points and residual activity was determined by measuring the initial rates of paraoxon hydrolysis. Residual activity at each time point was determined, and the relative activity compared to a sample incubated without the chelator was calculated. Data were fit to a single exponential decay curve: $A_t = A_0 e^{-kt}$,

where A_t corresponds to the residual activity after incubation for a given time, t, and A_0 is the activity at time zero, and *k* is the rate constant for inactivation

Expression and purification of recombinant hSIRT6 and dSIRT6

The dSIRT6 gene was synthesized by GenScript **(Data S2)** and cloned into pMAL C2x. pMAL plasmids carrying the genes hSIRT6 and dSIRT6 were transformed into Rosetta *E. coli* competent cells. Cells were grown at 37°C in TB medium containing ampicillin and chloramphenicol to A_{600}=0.6 and induced with 0.1 mM IPTG followed by 16 h incubation at 16°C. Cells were lysed using a French Press in lysis buffer (20 mM Tris-HCl pH 7.5, 100mM NaCl, and EDTA free-protease inhibitor cocktail (Calbiochem)). Cell debris was removed by centrifugation at 16,000g at 4°C for 40 min. The supernatants were loaded onto a pre-equilibrated amylose column eluted with elution buffer (20 mM Tris-HCl, 100 mM NaCl and 20 mM maltose pH 7.5). Protein purity was assessed by SDS-PAGE. The protein concentration was determined by the BCA method using bovine serum albumin as the standard.

Fluor de lys activity assay for SIRT6

Lysine-myristoylated TNFα peptide was conjugated to 4-amino-7-methylcoumarin group (AMC) at its C terminus (Peptron, Daejeon, South Korea). The fluor de lys activity assay was performed as described before(Wegener et al., 2003). Briefly, purified hSIRT6 and dSIRT6 were incubated at 37°C in reaction buffer containing 12.5 mM NAD+ and 1.25 mM TNFα myr-AMC peptide in assay buffer (50 mM Tris-HCl pH 8.0, 137 mM NaCl, 2.7 mM KCl, 1 mM MgCl2, 1 mg/ml BSA). At each time point, a 50µl aliquot was removed and mixed with 50µl of the developer solution (assay buffer+50 µM of HCl, 3 mg/ml trypsin and 10 mM nicotine amide). The quenched samples were kept at 37°C for 20 min prior to fluorescence measurements. Fluorescence readings were obtained using the TECAN infinite series 200 fluorimeter with excitation at 360nm and emission at 460nm in black 96-well solid plates (Greiner).

SIRT6 expression and activity in mammalian cell cultures

HEK293T and U2OS cell lines were obtained from the American Type Culture Collection. SIRT6 KO U2OS were generated using CRISPR-Cas9 gene disruption. Lentiviruses bearing SIRT6 CRISPR guiding sequence were produced in HEK293T cells and used to transduce

U2OS cells. Virally transduced cells were selected by the addition of 1 μg/ml puromycin (Sigma). All cells were grown in Dulbecco's modified Eagle's medium supplemented with 10% FBS, 100U/ml penicillin, 100mg/ml streptomycin and 2mM L-glutamine (all purchased from Biological Industries, Israel) and maintained at 37ºC under with 5% CO2.

Antibodies against SIRT6, H3, β-actin, and H3K56Ac were purchased from Abcam. An anti-FLAG antibody was purchased from Sigma.

Human SIRT6-FLAG variants cDNA sequences were cloned into pWZL-hygro for stable or transient transfection. Trans IT-LT1 (Mirus) was used to transfect HEK293T cells according to the manufacturer's protocol. Retroviruses bearing SIRT6-FLAG variants were produced in HEK293T cells and used to transduce a U2OS SIRT6 KO cell line. Virally transduced cells were selected for by the addition of 200μg/ml hygromycin B (Gold Biotechnology).

SIRT6 quantification by Western blot

Equal band areas on the Western membrane were used to measure the band intensities of hSIRT6, E1 and dE1 using the ImageJ software. Equal empty membrane areas around the bands were used to measure background intensities that were then subtracted from the band intensity values. The obtained values were normalized to actin levels by application of the same quantification method.

Expression and purification of Dnmt3a catalytic domains

Expression was performed essentially as described(Gowher and Jeltsch, 2001). Briefly, plasmids (peT28a) encoding hDnmt3a and dDnmt3a constructs were transformed into BL21(DE3)codon+ RIL cells. Bacteria were grown in TB medium. Protein expression was induced by addition of 0.5 mM IPTG. Following growth for another 13 h at 20°C, bacteria were harvested by centrifugation, washed with 100 mM NaCl, 1 mM EDTA, 10 mM Tris/HCl pH 8.0, and frozen at −20°C. Cells were lysed by sonication and the lysate was clarified by centrifugation for 1 h at 4°C, 20,000 rpm. The enzyme was purified on Ni-NTA agarose beads (Qiagen) at 4°C, eluted with 220 mM imidazole and dialyzed against 20mM Hepes, 200mM KCl, 0.2mM DTT, 1mM EDTA, 10% glycerol, pH 7.0. Due to the presence of contaminating bands, hDnmt3a and dDnmt3a concentrations were estimated by comparing their SDS-PAGE gel bands to various known amounts of bovine serum albumin (BSA).

Dnmt3a DNA-methylation assay

Methylation rates were measured with tritium-labeled SAM (2 μM), substrate DNA (509 bp biotinylated-DNA substrate containing 58 GpC sites; 0.4μM) and purified enzymes (0.32μM) essentially as described(Roth and Jeltsch, 2000). Aliquots taken at various time points were quenched by and transferred to streptavidin-coated ScintiPlate wells (PerkinElmer) and H^3 levels were determined using the Wallac MicroBeta TriLux counter (Perkin Elmer).

Myocilin-OLF expression, purification and thermal stability

dMyoc-OLF was synthesized and cloned into a pMal-c4x vector by GenScript **(Data S2)** utilizing MBP as a fusion protein for enhanced solubility, and a short amino acid linker as described previously for wild-type myoc-OLF(Burns et al., 2011, 2010). Fidelity of the plasmid was confirmed by DNA sequencing (MWG Operon). *E. coli* expression, purification, and cleavage from MBP, as well as determination of T_ms in 10mM Hepes pH 7.5, 200mM NaCl using differential scanning fluorimetry, were performed as described previously(Burns et al., 2011, 2010; Donegan et al., 2012).

Literature

Aricescu, A.R., Lu, W., Jones, E.Y., 2006. A time- and cost-efficient system for high-level protein production in mammalian cells. Acta Crystallogr. D. Biol. Crystallogr. 62, 1243–50. doi:10.1107/S0907444906029799

Berman, H. a., Leonard, K., 1989. Chiral reactions of acetylcholinesterase probed with enantiomeric methylphosphonothioates. Noncovalent determinants of enzyme chirality. J. Biol. Chem. 264, 3942–3950.

Burns, J.N., Orwig, S.D., Harris, J.L., Watkins, J.D., Vollrath, D., Lieberman, R.L., 2010. Rescue of glaucoma-causing mutant myocilin thermal stability by chemical chaperones. ACS Chem Biol 5, 477–487. doi:10.1021/cb900282e

Burns, J.N., Turnage, K.C., Walker, C.A., Lieberman, R.L., 2011. The stability of myocilin olfactomedin domain variants provides new insight into glaucoma as a protein misfolding disorder. Biochemistry 50, 5824–33. doi:10.1021/bi200231x

Chen, V.B., Arendall, W.B., Headd, J.J., Keedy, D.A., Immormino, R.M., Kapral, G.J., Murray, L.W., Richardson, J.S., Richardson, D.C., 2010. MolProbity: All-atom structure validation for macromolecular crystallography. Acta Crystallogr. Sect. D Biol. Crystallogr. 66, 12–21. doi:10.1107/S0907444909042073

Cherny, I., Greisen, P., Ashani, Y., Khare, S.D., Oberdorfer, G., Leader, H., Baker, D., Tawfik, D.S., 2013. Engineering V-type nerve agents detoxifying enzymes using computationally focused libraries. ACS Chem. Biol. 8, 2394–2403. doi:10.1021/cb4004892

Cheung, J., Rudolph, M.J., Burshteyn, F., Cassidy, M.S., Gary, E.N., Love, J., Franklin, M.C., Height, J.J., 2012. Structures of human acetylcholinesterase in complex with pharmacologically important ligands. J. Med. Chem. 55, 10282–10286. doi:10.1021/jm300871x

Donegan, R.K., Hill, S.E., Turnage, K.C., Orwig, S.D., Lieberman, R.L., 2012. The glaucoma-associated olfactomedin domain of myocilin is a novel calcium binding protein. J. Biol. Chem. 287, 43370–43377. doi:10.1074/jbc.M112.408906

Ellman, G.L., Courtney, K.D., Andres, V., Featherstone, R.M., 1961. A new and rapid colorimetric determination of acetylcholinesterase activity. Biochem. Pharmacol. 7, 88–95. doi:10.1016/0006-2952(61)90145-9

Emsley, P., Cowtan, K., 2004. Coot: Model-building tools for molecular graphics. Acta Crystallogr. Sect. D Biol. Crystallogr. 60, 2126–2132. doi:10.1107/S0907444904019158

Evans, P., 2006. Scaling and assessment of data quality, in: Acta Crystallographica Section

D: Biological Crystallography. pp. 72–82. doi:10.1107/S0907444905036693

French, S., Wilson, K., 1978. On the treatment of negative intensity observations. Acta Crystallogr. Sect. A 34, 517–525. doi:10.1107/S0567739478001114

Gowher, H., Jeltsch, A., 2001. Enzymatic properties of recombinant Dnmt3a DNA methyltransferase from mouse: the enzyme modifies DNA in a non-processive manner and also methylates non-CpA sites. J. Mol. Biol. 309, 1201–1208. doi:10.1006/jmbi.2001.4710

Grass, G., Fan, B., Rosen, B.P., Franke, S., Nies, D.H., Rensing, C., 2001. ZitB (YbgR), a member of the cation diffusion facilitator family, is an additional zinc transporter in Escherichia coli. J. Bacteriol. 183, 4664–7. doi:10.1128/JB.183.15.4664-4667.2001

Leslie, A.G.W., Powell, H.R., 2007. Evolving Methods for Macromolecular Crystallography, Evolving Methods for Macromolecular Crystallography. doi:10.1007/978-1-4020-6316-9

McCoy, A.J., 2006. Solving structures of protein complexes by molecular replacement with Phaser, in: Acta Crystallographica Section D: Biological Crystallography. pp. 32–41. doi:10.1107/S0907444906045975

Murshudov, G.N., Vagin, A.A., Dodson, E.J., 1997. Refinement of macromolecular structures by the maximum-likelihood method. Acta Crystallogr. Sect. D Biol. Crystallogr. doi:10.1107/S0907444996012255

Roodveldt, C., Tawfik, D.S., 2005. Directed evolution of phosphotriesterase from Pseudomonas diminuta for heterologous expression in Escherichia coli results in stabilization of the metal-free state. Protein Eng. Des. Sel. 18, 51–58. doi:10.1093/protein/gzi005

Roth, M., Jeltsch, a, 2000. Biotin-avidin microplate assay for the quantitative analysis of enzymatic methylation of DNA by DNA methyltransferases. Biol. Chem. 381, 269–72. doi:10.1515/BC.2000.035

Segel, I.H., 1976. Biochemical Calculations, 2nd Edition, John Wiley and Sons Inc, NY. doi:10.1016/0307-4412(76)90087-X

Sussman, J.L., Harel, M., Frolow, F., Varon, L., Toker, L., Futerman, A.H., Silman, I., 1988. Purification and crystallization of a dimeric form of acetylcholinesterase from Torpedo californica subsequent to solubilization with phosphatidylinositol-specific phospholipase C. J Mol Biol 203, 821–823.

Wegener, D., Wirsching, F., Riester, D., Schwienhorst, A., 2003. A Fluorogenic Histone Deacetylase Assay Well Suited for High-Throughput Activity Screening. Chem. Biol.

10, 61–68. doi:10.1016/S1074-5521(02)00305-8